System Level Performance of Cellular WiMAX IEEE 802.16 with SDMA-enhanced Medium Access[1]

Ralf Pabst, Jan Ellenbeck[2], Marc Schinnenburg, Christian Hoymann

RWTH Aachen University, Faculty 6, Chair of Communication Networks, Germany
EMail: pab@comnets.rwth-aachen.de

***Abstract*— Recent years have witnessed an ever-increasing interest in smart antenna technologies to boost the capacity of existing and future wireless systems. As one of the first standards the wireless metropolitan area network IEEE 802.16 (WiMAX) provides means to support these techniques. This paper investigates the potential of smart antenna beamforming and Space Division Multiple Access (SDMA) in the context of a cellular IEEE 802.16 deployment. It presents the system level performance evaluation of a joint TDMA/SDMA scheduling approach taking into account the influence of intra- and inter-cell interference generated by concurrent SDMA transmissions. The performance of single- and multi-user beamforming is compared with the non-beamforming reference case.**

I. Introduction

Recent years have witnessed an ever-increasing interest in smart antenna technologies to boost the capacity of existing and future wireless systems. As one of the first standards the wireless metropolitan area network IEEE 802.16 standard (further referred to as WiMAX (Worldwide Interoperability for Microwave Access)) provides means to support these techniques. Incorporating them into an SDMA-capable WiMAX base station (BS) not only requires antenna array and advanced signal processing facilities but also calls for extensions to the Medium Access Control (MAC) protocols, as described in [1]. Scheduling multiple users jointly in space and time leads to complex algorithms. The approach taken in this paper is to separate the joint scheduling into two distinct steps: (i) the spatial grouping of users that can be served in parallel using different beams and (ii) the scheduling of the resulting groups of users by means of well-known and well-researched scheduling algorithms in the time domain.

The approach to build spatial groups of users has also been proposed in previous publications. In [2] *Fuchs, Del Galdo and Haardt* propose a grouping algorithm for multi user Multiple Input Multiple Output (MIMO) systems which also computes groups that are then to be served in different time or frequency slots. The authors of [3] propose to construct intelligent space-time frames under the constraint of requiring a minimum signal-to-interference-plus-noise ratio (SINR) for each user, which implicitly leads to a grouping of users for parallel transmission in one time slot, too. In [4] *Koutsopoulos et al.* examine the impact of beamforming capable antennas on channel allocation at the MAC layer. Time/Code and Orthogonal Frequency Division Multiple Access (TDMA/CDMA and OFDMA) schemes are discussed and greedy heuristics are used to assign users to spatial channels. *Yin and Liu* [5] improve a greedy scheduling strategy introduced in [3] to also take several Quality of Service (QoS) parameters into account. The Ph.D. thesis [6] by *Bartolomé Calvo* gives a good overview of the literature in this field. The spatial grouping algorithm used in this work has been developed at the Chair of Communication Networks (ComNets) based on [2] and is described in [7], see also II. The contribution of this work is the performance evaluation of a proposed combination of spatial grouping and subsequent group scheduling in a multi-cellular scenario, taking into account the inter-cell interference from concurrent beams in adjacent cells.

The remainder of this paper is organised as follows: Section II introduces the system model, focusing on the joint application of spatial grouping of mobile users, SDMA beamforming and scheduling.

Next, Section III describes the multi cellular simulation scenario and all related assumptions. In Section IV we present the results of our dynamic, event-driven, stochastic simulations. Section V concludes the paper and gives an outlook on future work.

II. System Model

A. Smart Antenna Applications

The beamforming unit of our WiMAX BS is able to serve k users in parallel by forming beam patterns tailored to each combination of desired and undesired users. The beamforming algorithm applied is the *Optimal Beamformer* as described in [8]. For reference, consider Fig. 1. The green beam pattern is that of a conventional omnidirectional antenna. It emits the same amount of energy into all directions. The beamforming patterns in contrast, only radiate the full energy into the direction of the desired user. In all other directions, the emitted power is significantly reduced or even close to zero. This is advantageous both in Rx and Tx mode. When the beamforming station is receiving, it still gets the same desired signal strength, but collects significantly less interference from other directions because these are filtered through the beam pattern. Thus, the SINR value as the ratio of signal and interference power, is increased due to lower interference power. While

[1]This work has been funded by the European Commission in the projects WINNERII (IST-4-027756) and FIREWORKS (IST-27675 STP).

[2] Jan Ellenbeck is now with Munich University of Technology, Institute of Communication Networks

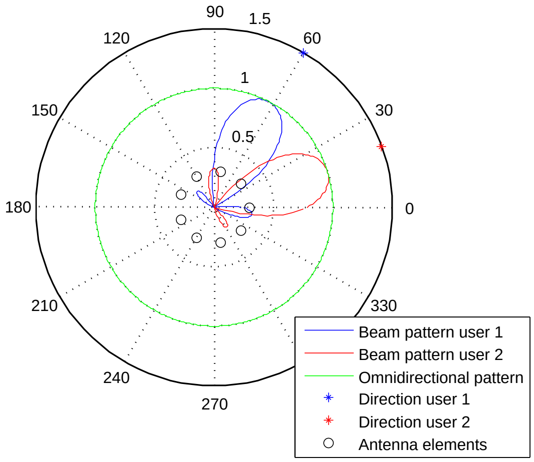

Fig. 1. Radiation pattern for 9-element circular antenna arrays (algorithm, see: [8])

transmitting, the station itself has no direct advantage because the same power will arrive at the receiving user. Here, the advantage is on the side of other users who see the station as a source of interference. Because the emitted power into other directions is reduced by the pattern, other users may achieve higher SINR values.

In our simulations, we investigate two different applications of beamforming antennas. The first is Spatial Filtering for Interference Reduction (SFIR), which means serving only one user at a time but with a suitable beam pattern. Even in this case, which does not require any modifications to the MAC protocol the use of beamforming is considered beneficial due to the reduction in emitted and received interference from other cells. This technique is often proposed to reduce cluster sizes in cellular systems.

The second application is SDMA operation, which denotes the possibility for multiple, spatially separable users to access the medium at the same time, on the same frequency, and within the same area (i.e. a cell). If the right beam patterns are used – having high gains in the direction of the desired users and signal suppression in the directions of other users – each user will receive a strong signal and only weak intra cell interference from the users served in parallel. An example of an SDMA transmission to 2 users is given in Fig. 1: User 1 (located at an azimuth angle of $60°$) and user 2 (located at an azimuth angle of $20°$) can be served simultaneously because each user's pattern has a null set in the other user's direction. In the uplink (UL), when users 1 and 2 are concurrently transmitting to the beamforming station, *joint detection* techniques of the beamforming system allow the parallel reception. Fig. 2 summarizes how the different transmission techniques (omnidirectional antennas, SFIR, and SDMA) can be used by the base stations in a clustered cellular deployment.

B. Joint TD-/SDMA Scheduling

This section gives an overview of our concept for combined TD-/SDMA packet scheduling. As indicated in the introduction, our approach separates the scheduling into two stages. In a first step, an SDMA scheduling is performed by what we call a spatial grouper. The grouping process will be briefly described in the first part of this section. In the second half, we will describe how the result of the first step – the spatial grouping of co-scheduled users – is taken as an input for the TDMA scheduling process.

We first compute a spatial grouping of users that can be well separated by the base station's beamforming antenna. The result of this grouping is a set of spatial groups of users. The users of a group can be served on the same frequency band at the same time. For users from distinct groups this separability is not given so that different groups have to be separated in the time domain. Consequently, the resulting spatial groups are scheduled onto time resources using a well-known scheduling method.

In mathematical terms, a spatial grouping is a partition $\mathcal{P}$ of the set of all users U. That is, every user u_i belongs to exactly one spatial group G_j. These spatial groups are both collectively exhaustive (refer to (4)) and mutually exclusive (refer to (5)) with respect to the set of all users:

$$
\begin{aligned}
U &= \{u_1, u_2, ..., u_n\} && (1)\\
G_j &\subseteq U && (2)\\
\mathcal{P} &= \{G_1, G_2, ..., G_j, ...\} && (3)\\
U &= \bigcup_{G_j \in \mathcal{P}} G_j && (4)\\
G_i \cap G_j &= \emptyset \quad \text{for } i \neq j && (5)
\end{aligned}
$$

For our purposes, not every possible partition should be allowed as a valid grouping. On the one hand, the smart antenna system supports only a limited number of concurrent beamforming transmissions. If we denote the maximum number of supported beams with k, only partitions $\mathcal{P}$ whose elements (subsets) G_j have cardinalities that are limited by k, i.e., $|G_j| \leq k \quad \forall G_j \in \mathcal{P}$ are allowed. On the other hand, a partition is invalid if it leaves a user unserved. This might occur when users that are not well separable are grouped together. In this case, the mutual interference might become so high that one or several users perceive an SINR that is not sufficient for successful data transmission. Considering such a grouping would contradict our main objective to achieve high system throughput while serving all users. The grouping algorithm used is a tree-based heuristic operating on estimated SINR values. A detailed presentation as well as a performance and complexity analysis can be found in [7].

After completing the spatial grouping, the resulting groups are scheduled in the time-domain using a Proportional Fair Scheduler. It aims to offer a trade-off between fairness and throughput. The throughput optimization over e.g. Round Robin schedulers is realized by preferring groups of users for which the grouper has estimated high SINR values, thus promising high throughput. The fairness is achieved by also taking into account the past data rates that the users have experienced. This way, not only groups that promise above average throughput in the future, but also those that have experienced below average throughput in the past, are preferred.

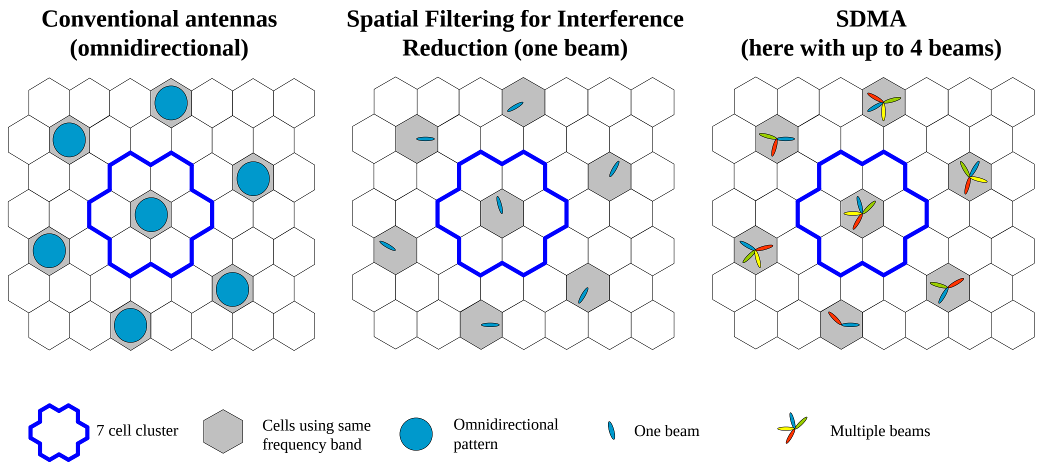

Fig. 2. Comparison of a 7 cell cluster with omnidirectional and beamforming antenna in SFIR and SDMA mode. Adapted from [9].

The preference value of a user is usually defined by the ratio of its future and past data rates. In our case again, we have to adapt this to scheduling groups of users. The future data rate of a group is easily derived from the estimated data rates of the group members. Determining the past data rate is much more difficult. The reason is that groupings may change on a frame-to-frame basis. So the members of a current group may have belonged to different groups in the past. If the average of the members' past data rates was chosen, it would be possible for high data rate users to starve out users with low data rates. Therefore, we use the group's total future throughput and the minimum past group member throughput for computing the ratio to maximize:

$$preference(G_j) = \frac{\sum_{u \in G_j} EstimatedDataRate(u)}{1 + \beta \min_{u \in G_j} \{PastDataRate(u)\}} \quad (6)$$

This ratio is computed for every spatial group G_j obtained from the grouper. The groups are then served in order of descending ratios. The factor β determines how much influence the past data rates have on the group's preference. The algorithm we have implemented uses $\beta = 1$ and updates the past data rates using an exponential smoothing technique, thus weighting older data rates with exponentially decreasing weight values:

$$PastAvgRate_t = \alpha\, CurrentRate + (1-\alpha)\, PastAvgRate_{t-1}$$
$$0 \leq \alpha \leq 1 \quad (7)$$

III. Simulation Scenario

The evaluated scenario consists of 7 cells, each with a central base station and 25 subscriber stations. The locations of the base and subscriber stations are shown in Fig. 3. Their positions remain unchanged for all simulations that are conducted. Measurements are only performed in the central cell (black) for the corresponding BS and SSs. The stations in the surrounding 6 cells only produce interference for the central cell and are not evaluated. Nevertheless, the same event driven stochastic simulation, with identical average traffic loads, and with the same degree of detail, is conducted at all 182 stations.

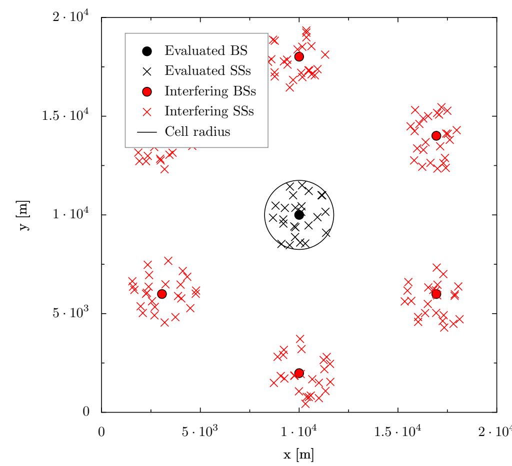

Fig. 3. Positions of BSs and SSs in central (black) and co-channel (red) cells of evaluated clustered cellular deployment

The cells have a radius of $R = 1750\,m$ and an $N = 7$ cell cluster order is used as shown in Fig. 2. The cells not shown are assumed to operate on different frequency bands, which means their interference can be ignored. The nearest interfering cells (colored red) have a distance of $D = \sqrt{3N}\,R = 8020\,m$. Cluster order and cell radius have been selected based on *Matlab* calculations such that a user at the cell border will perceive an SINR $\geq 6.4\,dB$ during MAP reception (for SINR thresholds see table I). As the cells are synchronized, all base stations transmit their DL and UL MAPs at the same time. They have to use an omnidirectional broadcasting pattern which means that the users experience worst case SINR levels during these times. Thus, all SSs in our simulations are guaranteed to be within coverage of their BS all the time.

A. Simulator and traffic model

The Wireless Network Simulator (WNS) developed at ComNets is a time discrete, event driven simulator. The load generator of each station generates IP data packets according to a specified arrival process and feeds them into the WiMAX data link layer (DLL) via the suitable Service Access Point (SAP). When a packet is scheduled, it is forwarded to the physical layer (PHY) module that adds the packet's transmission to the set of currently active transmissions in the scenario. Until the transmission is over, all other packets transmitted at the same time on the same frequency band will experience the interference generated by the transmission, taking into account pathloss and the antenna characteristics in form of the beam pattern. As we examine the performance – measured as cell throughput, delay, etc – for a certain traffic load, the inter arrival time (IAT) and the packet size have to be chosen accordingly. In all simulations we assume a fixed packet size of 1024 Bits or 128 Bytes. Thus, we have to adapt the IAT so that the desired traffic load results for the cell. We assume the IAT, with which packets arrive at the WiMAX MAC layer, to follow a negative exponential distribution.

For all subscriber stations we apply symmetric traffic loads in DL and UL direction to and from all users. Thus, to achieve a total (DL + UL) cell traffic load of $Traffic$, we have to set the IAT to the following mean value:

$$IAT[s] = \frac{\#(SS) * PacketSize * 2}{Traffic} \quad \frac{[Bit]}{[Bit/s]} \tag{8}$$

To evaluate the performance of a specific beamforming application with respect to the offered traffic, we conduct a number of independent simulation runs, varying the IAT. For each run, the following performance values are derived and evaluated:

Throughput: Measured in Bit/s as the total bits of all packets successfully arriving at the WiMAX SAP of the destination station during a fixed time window. Separate values are measured for packets traveling to/from every SS in UL and DL direction.

Delay: Measured at the destination station's WiMAX SAP for all packets that have been successfully transmitted. Defined as the time elapsed between entering the sender's WiMAX protocol layer until leaving it at the destination's WiMAX SAP. In particular, all delays experienced in buffers are counted. It should be kept in mind that under overload conditions, the mean delay values are only partly meaningful. The reason is that the infinite delay of packets that are never transmitted is neither included in mean values nor counted because these packets never reach the destination's WiMAX SAP. The delay figures are always given in seconds.

SINR: Measured in dB as the ratio of the transmission's carrier power and the sum of interference and noise at the receiver.

B. Link adaptation and error modeling

The scheduling strategy performs link adaptation based on the SINR estimations provided by the spatial grouper. For each packet that is scheduled for transmission to a subscriber station, a modulation and coding scheme (MCS) (also referred to as PHY-mode) with the respective PHY data rate is chosen according to the SINR threshold values shown in table I. These values are taken from the IEEE 802.16 WiMAX standard [10]. The SINR threshold values aim at a target residual bit error rate (BER) of 10^{-6}.

TABLE I

MCS SWITCHING THRESHOLDS AND PHY DATA RATES

#	Modul.	R_c	SINR$_{\min}$ $[dB]$	PHY data rate $[MBit/s]$
1	BPSK	1/2	6.4	6.91
2	QPSK	1/2	9.4	13.82
3	QPSK	3/4	11.2	20.74
4	16 QAM	1/2	16.4	27.65
5	16 QAM	3/4	18.2	41.47
6	64 QAM	2/3	22.7	55.30
7	64 QAM	3/4	24.4	62.21

In order to avoid transmission errors, the SINR thresholds are chosen very conservatively with respect to the assumed SINR – BER mapping. Thus, as long as the SINR estimations deliver accurate values, transmission errors are kept to a minimum in our simulations. The downside is that, in some cases, higher throughput values could be reached if the link adaptation was more aggressive.

C. WiMAX frame structure and overhead

In our simulations the total frame duration is assumed to be 10 ms. We divide this time equally between DL and UL data transmission phases. UL and DL MAPs are always transmitted using an omnidirectional antenna pattern. Beamforming for SFIR or concurrent SDMA transmissions are only used for the DL and UL bursts. When operating in SDMA mode, the base station can schedule multiple concurrent bursts and has to set beam patterns accordingly to separate the co-scheduled users' signals. Of course, individual MAP entries (information elements, IEs) for parallel bursts have to be signaled.

No OFDMA is used, i.e., the 192 data carriers available in the 20 MHz bandwidth are grouped into a single frequency channel. Each OFDM symbol is 13.89 10^{-5} seconds long, making for a total of 720 OFDM symbols in each 10 ms frame [11]. Each MAP is transmitted using BPSK $1/2$ as the modulation and coding scheme. Using 192 data carriers, 96 bits can be transmitted with one symbol. Thus, an UL MAP holding 25 information elements is 14 full OFDM symbols long (1.94% of the frame). A DL MAP holding 75 information elements needs 39 symbols (5.4% of the frame). 7 OFDM symbols are deducted from the frame capacity to account for the different phases of the preamble. In total, the organizational overhead for the whole frame is 8.3%.

D. Other Simulation parameters

We use the combined TD-/SDMA scheduler only at the base station. For the uplink, a simple Round Robin scheduling strategy has been used for bandwidth reservation purposes in the base station. The results section will therefore focus on the DL only. In the SSs, a simple scheduler was used. In order to rule out other influencing factors when evaluating the scheduler's performance, neither Segmentation and Reassembly (SAR) nor Automatic Repeat Request (ARQ) mechanisms are used.

Each base station is equipped with a 9-element uniform circular antenna array used to serve the whole cell without

TABLE II

OVERVIEW OF SIMULATION PARAMETERS

Parameter	Value (Comment)
Antenna array	Uniform Circular Array (Only at the BS)
Antenna elements	9
Transmit power	1 Watt (Both BS and SS)
Cluster size	7 (One tier of interferers)
Stations per cell	25
Cell size (radius)	1750 $[m]$ (Aligned for BPSK 1/2 at the cell border)
Mid frequency	5.470 GHz (CEPT band B)
Bandwidth	20 MHz
Pathloss	WINNER LOS C.1 Metropolitan SubUrban single-slope, see (9)
Traffic model	Symmetric
Packet size	1024 Bit (Fixed)
Inter arrival time	see section III-A
Frame length	10 ms (720 OFDM symbols)
Data carriers	192 (Available for data transmission)
Sub bands	1 (All data carriers form one frequency channel)
OFDM Symbol duration	13.89 μs
Fixed UL MAP overhead	25 symbols
Fixed DL MAP overhead	75 symbols
Misc. overhead	7 symbols (For FCH, preambles, RTG and TTG)
SAR	None
ARQ	None

sectorization. The SSs are equipped with standard omnidirectional antennas. For both station types, the transmit power is 1 Watt and no further power control / adaption is performed. A bandwidth of 20 MHz with a mid frequency of 5.470 GHz is used.

The stations, including the subscriber stations, are assumed to be fixed at the positions depicted in Fig. 3. As a roof-top deployment for the subscriber station's antenna is envisioned, the pathloss model presumes LOS conditions. The "C1 LOS" pathloss model for a suburban environment as derived by the Wireless World Initiative New Radio (WINNER) project is used in the following. According to the model, which is based on measurements, the pathloss for a receiver in a distance of d meters can be approximated to: [12]

$$Loss(d) = 23.8 \log(d/[m]) + 41.9 \, [dB] \tag{9}$$

Shadowing or fading effects are not considered. Table II gives an overview of all relevant simulation parameters.

IV. SIMULATION RESULTS

In this section, we present and discuss the results of the performed simulations. First, we will discuss throughput and delay values for the three different transmission modes: (i) omnidirectional (ii) SFIR and (iii) SDMA.

Fig. 4 shows the aggregate DL cell throughput versus the offered traffic load. As expected, saturation load values increase when shifting from omnidirectional to SFIR and SDMA transmission. For the omnidirectional and the SFIR case, the final saturation levels are not much higher as the points at which the respective throughput curves deviate from the offered traffic. In the SDMA case with up to 4 concurrent transmissions, the throughput curve climbs from a value of

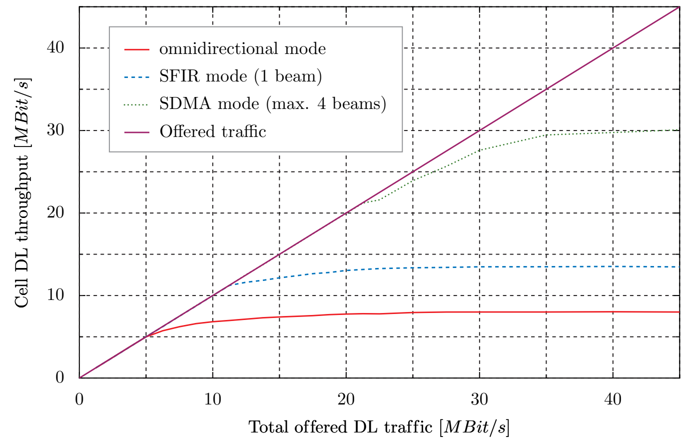

Fig. 4. Comparison of DL throughput vs. total offered DL traffic for omnidirectional, SFIR, and SDMA transmission modes

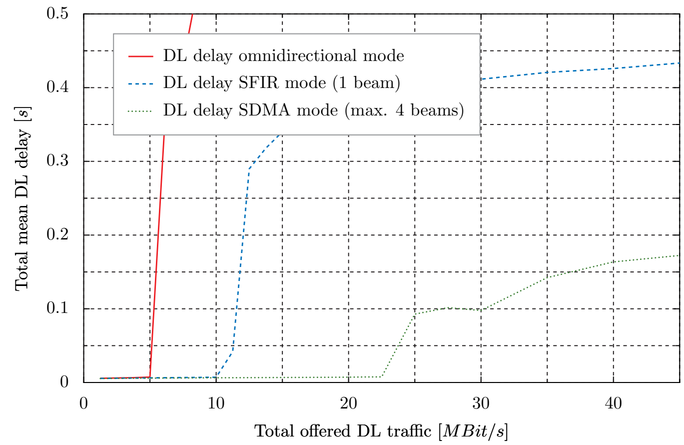

Fig. 5. Comparison of mean DL delay vs. total offered DL traffic for omnidirectional, SFIR, and SDMA transmission modes

about 22 $MBit/s$, when the first users reach saturation, to a final saturation throughput of 30 $MBit/s$. Taking the points when the first users reach saturation as a reference, the SFIR transmission achieves a gain of 240% as compared to the omnidirectional case. The SDMA transmission with up to 4 beams achieves a gain of more than 80% as compared to the SFIR transmission. When compared with the omnidirectional transmission, it reaches an even higher gain of 440%. This result is backed quite well by Fig. 5, which compares the mean DL packet delay versus increasing traffic load for the three transmission modes. The different saturation load levels match those observed in Fig. 4.

Next we discuss the CCDF of the experienced SINR values shown in Fig. 6. We can see that the positioning of the subscriber stations in our scenario results in a balanced mix of available SINR values ranging from about 7 dB to over 30 dB. All PHY-modes listed in table I are represented. The red curve (for omnidirectional transmission) also gives an indication about the distribution of SINRs during the MAP-reception for all 25 SSs. Each step represents one or several users with the same SINR. The SFIR mode exhibits an up to 8 dB advantage over the reference case due to the reduced

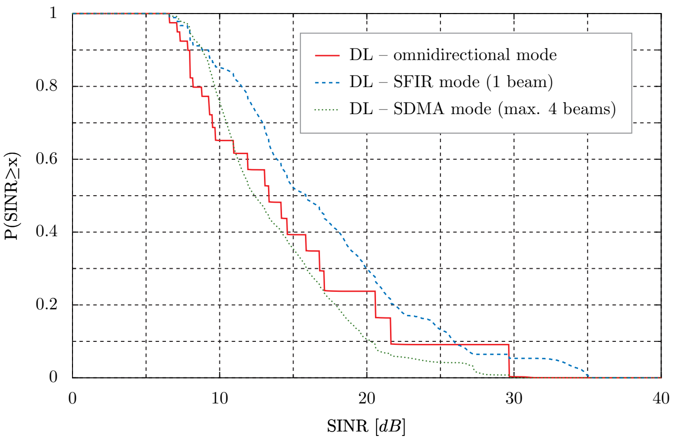

Fig. 6. CCDF of DL SINR values for different transmission modes at 50 $MBit/s$ offered traffic

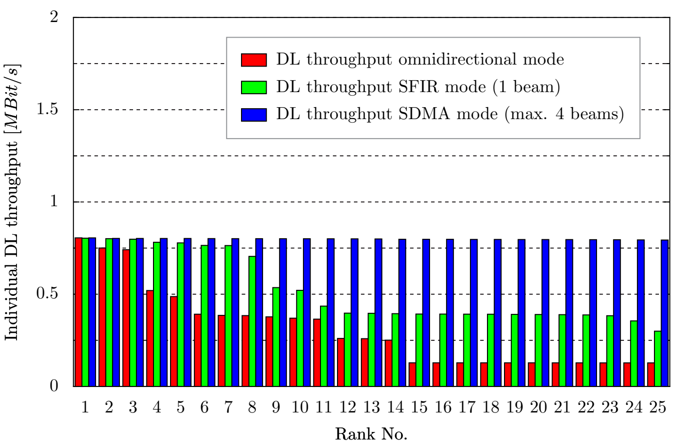

Fig. 7. Individual DL throughput of SSs (sorted in descending order) at 20 $MBit/s$ DL traffic

interference. The curve for the SDMA transmission with up to 4 beams partly runs below the omnidirectional curve. This is not primarily caused by additional interference but by the fact that the received signal power for the SDMA transmissions is sometimes lower than in the omnidirectional reference case: The beamformer's effort to avoid interfering co-scheduled users can lead to a gain smaller than 1 for the desired user. As the grouper is aware of that (it asks the PHY for an SINR estimation), it avoids this effect by not aggressively grouping users who already have a low SINR. As a consequence, the probability of having a certain minimal SINR level is higher for the SDMA case at low SINR levels.

To answer the question about the fairness of the described group scheduling process, Fig. 7 shows the distribution of the capacity added by transmitting in SFIR and SDMA over the SSs. The bars indicate each individual SS's throughput under a traffic offer of 20 $MBit/s$ DL traffic. As we have seen above, the system is in saturation for omnidirectional and SFIR mode. This leads to a somewhat unbalanced distribution of the individual throughput values since not all users in a spatial group may exploit their assigned transmission periods ideally. But still, even in overload condition, all users get a fair share of the overall resources. Naturally, in the SDMA case all users can be served to their full satisfaction because the MAC frame capacity is not yet exhausted under the considered load conditions.

V. Conclusion and Outlook

We have presented a simulative performance evaluation of a cellular WiMAX deployment which makes use of beamforming smart antennas and SDMA medium access. We proposed a combination of spatial user grouping and group scheduling to keep the computational complexity of the joint TDMA/SDMA scheduling process within reasonable bounds and have proven the feasibility of this concept through implementation in a system level simulation tool. Under the proposed fair scheduling, the investigated SFIR and SDMA schemes have proven to substantially increase the usable system capacity, even in a cellular system with inter-cell interference. The investigation has shown that the main limitation regarding the minimal cluster order stems from the low SINRs during MAP transmissions. Even when using beamforming these have to be performed using omnidirectional patterns. Thus, a tighter frequency re-use would require more intelligent MAP transmission strategies.

If the spatial grouping is constantly updated to reflect the current spatial distribution of subscribers the proposed two-stage joint TD-/SDMA scheduling concept also supports mobile SSs. It could therefore be used for IEEE 802.16e based systems, too.

References

[1] C. Hoymann, "MAC Layer Concepts to Support Space Division Multiple Access in OFDM based IEEE 802.16s," *Wireless Personal Communications*, p. 23, May 2006, dOI: 10.1007/s11277-005-9005-6. [Online]. Available: http://www.comnets.rwth-aachen.de

[2] M. Fuchs, G. Del Galdo, and M. Haardt, "A novel tree-based scheduling algorithm for the downlink of multi-user MIMO systems with ZF beamforming," in *Acoustics, Speech, and Signal Processing, 2005. Proceedings. (ICASSP '05). IEEE International Conference on*, vol. 3, 2005.

[3] F. Shad, T. Todd, V. Kezys, and J. Litva, "Dynamic slot allocation (DSA) in indoor SDMA/TDMA using a smart antenna basestation," *IEEE/ACM Transactions on Networking*, vol. 9, no. 1, pp. 69–81, 2001.

[4] I. Koutsopoulos, T. Ren, and L. Tassiulas, "The impact of space division multiplexing on resource allocation: a unified approach," in *INFOCOM 2003. Twenty-Second Annual Joint Conference of the IEEE Computer and Communications Societies. IEEE*, vol. 1, 2003, pp. 533–543.

[5] H. Yin and H. Liu, "Performance of space-division multiple-access (SDMA) with scheduling," *IEEE Transactions on Wireless Communications*, vol. 1, no. 4, pp. 611–618, 2002.

[6] D. Bartolomé Calvo, "Fairness Analysis of Wireless Beamforming Schedulers," Ph.D. dissertation, Universitat Politècnica de Catalunya (UPC), Department of Signal Theory and Communications, Nov 2004.

[7] C. Hoymann, J. Ellenbeck, R. Pabst, and M. Schinnenburg, "Evaluation of Grouping Strategies for an Hierarchical SDMA/TDMA Scheduling Process," in *Proceedings of ICC2007*, Glasgow, United Kingdom, to appear 2007.

[8] L. Godara, "Applications of antenna arrays to mobile communications. I. Performance improvement, feasibility, and system considerations," in *Proceedings of the IEEE*, vol. 85, no. 7, 1997, pp. 1031–1060.

[9] A. Molisch, *Wireless Communications*. John Wiley & Sons, Ltd., 2005.

[10] "IEEE standard for local and metropolitan area networks part 16: Air interface for fixed broadband wireless access systems," in *IEEE Std 802.16-2004 (Revision of IEEE Std 802.16-2001)*, 2004, pp. 1–857.

[11] C. Hoymann, "Analysis and Performance Evaluation of the OFDM-based Metropolitan Area Network IEEE 802.16," *Computer Networks, Selected Papers from the European Wireless 2004 Conference*, vol. 49, no. 3, pp. 341–363, Oct 2005.

[12] "**W**ireless World **In**itiative **Ne**w **R**adio," http://www.ist-winner.org.